International Journal of Chemical and Biomolecular Science
Vol. 1, No. 2, 2015, pp. 22-26
http://www.aiscience.org/journal/ijcbs

Determination of Bubble Size Distribution in Pressurized 3D Bubble Columns Using Borescope-Based Imaging Technique

Md. Iqbal Hossain[1, *], Raymond Lau[2], Yanhui Yang[2], Armando Borgna[3]

[1]Department of Chemical Engineering, Bangladesh University of Engineering and Technology, Dhaka, Bangladesh
[2]School of Chemical and Biomedical Engineering, Nanyang Technological University, Jurong, Singapore
[3]Division of Heterogeneous Catalysis, Institute of Chemical and Engineering Sciences, Jurong Island, Singapore

Abstract

The dynamic interactions between the gas and the liquid phases, irregularity in bubble shape, higher gas holdup, and high mechanical stress, etc at elevated pressures complicate the application of many techniques in bubble size measurement in bubble columns. In this study the feasibility of a new borescope-based imaging technique to determine the bubble size distribution in 3-dimensional bubble columns under elevated pressures is investigated assessing bubble size distribution over a range of superficial gas velocities and operating pressures. The observed size distribution results reveal that borescope-based imaging technique can be employed for the determination of bubble size distribution with reasonable accuracy in bubble columns under elevated pressures.

Keywords

Bubble Size Distribution, Bubble Columns, Elevated Pressure, Borescope

Received: May 7, 2015 / Accepted: June 1, 2015 / Published online: July 9, 2015

1. Introduction

Many chemical, biochemical, and petrochemical industrial processes employ bubble columns. The extensive knowledge of bubble properties such as gas holdup and bubble size distribution is crucial to the modeling, design and scale-up of bubble columns. The bubble size distribution governs the mass transfer interfacial area and the mass transfer rate is the controlling step of many chemical and biochemical processes.[1-4] Though the determination and study of gas holdup are readily available, the determination of bubble size distribution with high accuracy has always been a challenge especially in 3D bubble columns.[4] The determination of bubble size distribution in 3D bubble columns becomes more complicated and challenging under elevated operating pressures. The factors which make it more complicated and challenging are the higher gas holdup, dynamic interactions between the gas and liquid phases, and high mechanical stress, etc. However, under these conditions, the application of borescope in 3D bubble columns would allow direct visualization of the local bubble images. The size-distribution determination capability and accuracy of borescope integrated with a statistical reconstruction method and a depth-of-field model have already been successfully demonstrated in our previous studies performed in a liquid-solid system under ambient pressure only where the discrete solids were of fixed shape.[5, 6]Hence the feasibility of determining bubble size distribution using the borescope-based imaging technique is investigated in the present study in a more complicated and challenging dynamic, chaotic, and shape-irregular gas–liquid system (i.e., 3D bubble columns) under elevated pressure conditions.

* Corresponding author
E-mail address: iqbalhossain@che.buet.ac.bd (Md. I. hossain)

2. Experimental Section

The schematic diagram of the experimental setup is shown in Figure 1a. The column is made of stainless steel and workable at a maximum pressure of 100 bar and a maximum temperature of 350 ºC. The main column section has an internal diameter of 30 mm and a height of 218 mm. A perforated plate has a hole size of 1 mm in a triangular pitch pattern of pitch distance 4 mm is used as the gas distributor. Mass flow meters are installed at the inlet and outlet of the column to control the operating gas velocity and operating pressure. De-ionized (DI) water is used as the liquid phase and compressed nitrogen is used as the gas phase. The temperature is maintained at 20 ºC and the pressure is varied from 1bar to 10bar. An initial static liquid level of Z/D = 7.2 is maintained in the column section. The superficial gas velocity is varied from 20 mm/s to 50 mm/s. Sufficient time is allowed for each flow condition to reach steady state. A pressure transducer (Validyne DP-15) is installed to measure the pressure difference between 30 and 180 mm from the distributor plate. The gas holdup is determined based on the equation:[17, 18]

$$\varepsilon_G = \frac{\left(dP/dZ\right)_d}{g\left(\rho_L - \rho_G\right)} \tag{1}$$

where ε_G is the gas holdup, $\left(dP/dZ\right)_d$ is the dynamic pressure gradient measured between two axial heights,[17,18] g is the gravitational constant, ρ_G is the gas density and ρ_L is the liquid density.

A rigid borescope (Olympus) is coupled with a high speed video camera (Olympus I-speed) to record the local bubbles in the column. The bore scope is 5.8 mm in diameter and 250 mm in length with a 60º field of view and 0º direction of view. Modification of the borescope has been made to allow operation at risky elevated pressures. The maximum working pressure of the modified probe is 15bar. A high intensity light source (Olympus, ILP) is used to provide internal illumination to the borescope. The borescope is installed at 4 mm from the column wall and at an axial location, Z/D of 5.6. The borescope is adjusted with a focus plane 5 mm away from the probe tip. The magnification of a reference object at various distances from the borescope is reported in Hossain et al.[5] As a certain degree of distortion is present in the borescope image, corrections for distortion are made based on Haneishi et al.[7] A corrected sample borecsope image of bubbles is shown in Figure 1b.The bubble sizes are first measured from the borescope images in terms of pixel number. The pixel number is converted into linear dimension using calibration. Since most of the bubbles are not spherical shape, the feret (which is maximum linear dimension) diameter is used to represent the bubble size. A bubble sample size of 300 is used for each measured bubble size distribution.

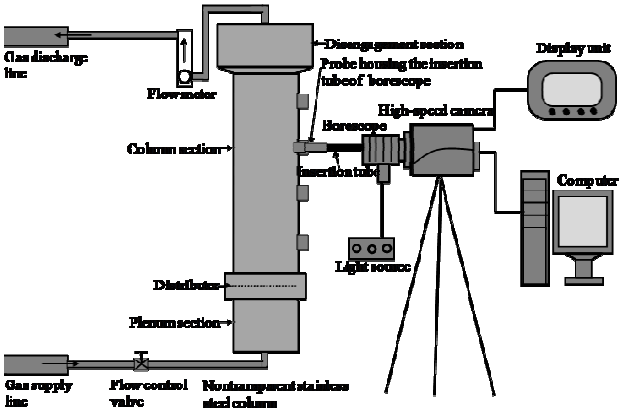

Figure 1 (a). Schematic diagram of the experimental setup.

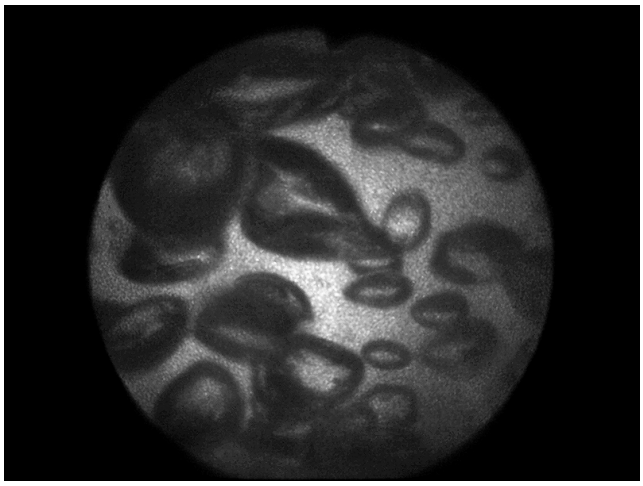

Figure 1 (b). A sample borescope image of bubbles in a bubble column.

A log-normal distribution is used in the reconstruction of the actual bubble size distribution from measured bubble size distribution by following Hossain et al.[5] The reconstruction of the actual bubble size distribution requires the depth-of-field (DOF) information. The DOF is determined based on the model developed in our previous study:[6]

$$\mathrm{DOF}_{c_{Critical-1}\le c\le c_{Critical-2}} = \mathrm{DOF}_{c\le c_{critical-1}}\left[1-\left(\frac{c-c_{Critical-1}}{c_{Critical-2}-c_{Critical-1}}\right)^n\right] \tag{2}$$

where $\mathrm{DOF}_{c\le c_{critical-1}}$ is the DOF of the borescope in the absence of obstruction and is determined by the initial setting and calibration test of borescope itself.[5,6] $c_{Critical-1}$ is the critical volume fraction of objects below which DOF remains constant and $c_{Critical-2}$ is the critical volume fraction of objects at maximum packing. In a gas–liquid system, the objects of interest are the bubbles and the volume fraction of objects is

therefore equivalent to the gas holdup, ε_G . $c_{Critical\text{-}1}$ and $c_{Critical\text{-}2}$ are determined experimentally as 0.07 and 0.61 respectively and the detail are available in Hossain et al.[6] Assuming DOF model linearity, $n = 1$ is used in this study.

3. Results and Discussion

3.1. Comparison with Literature Size Distribution Results

The reconstructed bubble size distribution obtained by borescope measurement is compared with three bubble size distributions reported in the literature. All the bubble size distributions are measured in the air–water system under ambient conditions at a superficial gas velocity of 20 – 30 mm/s. It is important to note that the various bubble size distributions reported are not presented in a unified size parameter. For example, the bubble size distribution reported in Wang et al. [8]and Kulkarni et al.[2] expressed the bubble size using volume-equivalent diameter while Xue et al.[4] presented the maximum cord length as the bubble size. Therefore, the bubble size distributions reported in Xue et al. and the current study are converted to volume-equivalent diameter before comparisons can be made. At a superficial gas velocity of 20 mm/s, the bubble column is expected to be operating in the dispersed–bubble regime and the bubbles are expected to have a uniform size and shape.[9]Based on visual observation, it is considered that all the bubbles are ellipsoidal shape and have aspect ratios of 1.6. As a result, the maximum cord length, essentially the minor axis of an ellipsoid, presented in Xue et al. and the feret diameter, the major axis of an ellipsoid, presented in the current study can be converted to volume equivalent diameter based on the volume of an ellipsoid with the respective minor and major axis and an aspect ratio of 1.6.

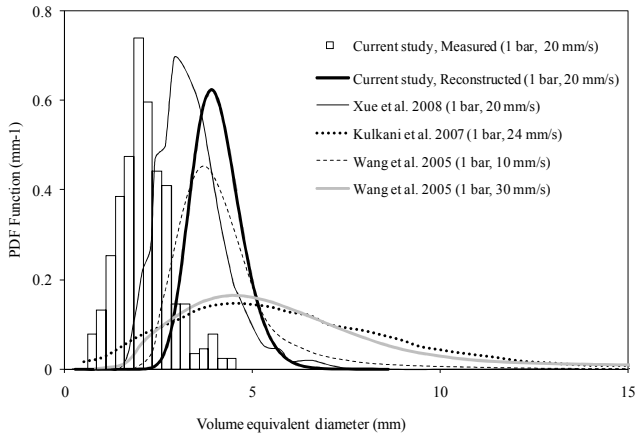

Figure 2. Comparison of borescope bubble size measurement with literature results.

A comparison of the converted bubble size distributions and their respective measurement conditions are shown in Figure 2. It can be seen that the bubble size distribution obtained in the current study is fairly similar to the one reported in Xue et al. There is a minor difference in the mean bubble size between the two bubble size distributions due to the difference in gas distributors used in these two studies. At a superficial gas velocity of 20mm/s, it is likely that the column is operated in the dispersed–bubble regime. There is little bubble coalescence in the dispersed–bubble regime and the bubble size is mainly governed by the orifice size of the gas distributor.[4] It is possible that the 0.5mm orifice diameter used in Xue et al. is generating a smaller bubble size distribution than the 1.0 mm diameter used in the current study. On the other hand, though the bubble size distribution reported in Kulkani et al. has similar mean bubble size as compared to that reported in the current study, the distribution is significantly wider. Despite the fact that the bubble size distribution reported in Kulkani et al. is measured at 24 mm/s, the wide bubble size distribution is indicating an operation in the coalesced–bubble regime. Further comparison with Wang et al. shows that the bubble size distribution at 24 mm/s reported in Kulkani et al. is rather similar to the bubble size distribution at 30 mm/s reported in Wang et al. At the same time, the bubble size distribution at 20 mm/s reported in this study coincides well with the bubble size distribution at 10 mm/s reported in Wang et al. Therefore, it is certain that the regime transition from the dispersed–bubble regime to the coalesced–bubble regime happens at a gas velocity of 24 mm/s. Nonetheless, the reasonable agreement of the bubble size distribution obtained in the current study with the bubble size distributions reported in literature has demonstrated the feasibility of determining bubble size distribution using the borescope-based imaging technique.

3.2. Comparison of Bubble Size Distribution at Different Pressures

Many bubble column applications are operated under elevated pressures. In general, an increase in the operating pressure causes the gas properties and other phenomena to change substantially. All these factors contribute to a change in the bubble behavior and bubble size distribution. The bubble size distributions including mean size (μ, mm) and variance (σ^2, mm^2, which is the wideness of size distribution) shown in Figure 3 are evaluated at a superficial gas velocity of 50 mm/s and operating pressures of 1 bar, 5 bar and 10 bar. It is to note that while the dispersed–bubble/coalesced–bubble regime transition velocity depends on a number of factors such as liquid and gas properties, column diameter, column height-to-diameter ratio, and distributor design, air–water systems are reported to have an experimental regime transition velocity range of 24 mm/s to 65 mm/s at ambient

pressure.[9-13] Based on the regime transition velocity correlation proposed by Reilly et al.,[9] the regime transition velocities at 1 bar and 10 bar can be estimated as 29 mm/s and 56 mm/s, respectively. Therefore, a bubble column can be considered to operate in the coalesced–bubble regime at a superficial gas velocity of 50 mm/s under ambient pressure. The wide bubble size distribution in Figure 3 is an indication of the coexistence of large and small bubbles. As the operating pressure is increased from 1 bar to 5 bar, the bubble size distribution becomes narrower. The probability of large bubble sizes decreases while the one of small bubble sizes increases. It is in agreement with the literature, which proves again the feasibility of borescope measurement, that an increase in the operating pressure suppresses the bubble coalescence and promotes the bubble breakup.[14,15] However, when the operating pressure is further increased from 5 bar to 10 bar, both the probabilities of large and small bubble sizes decrease. The suppression of bubble coalescence is reaching a point that there is no large bubble available to undergo bubble breakup. The bubble size distribution becomes so narrow that the bubble column can be considered to be operating in the dispersed–bubble regime. The result also indicates supporting the feasibility of borescope measurement that the regime transition velocity of 56 mm/s predicted by the correlation proposed by Reilly et al. gives indeed a reasonable estimation for the current system.

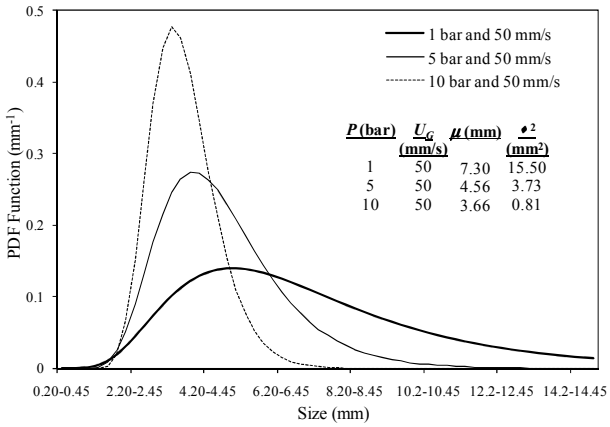

Figure 3. Comparison of bubble size distribution at a superficial gas velocity of 50 mm/s and various operating pressures.

3.3. Potential Errors in the Determination of Size Distribution

It is worthy to note that the borescope used in this study has a maximum viewable size limit of 6 mm at the focusing plane. The gas bubbles in air–water system under ambient pressure and superficial gas velocities higher than 50 mm/s are typically larger than 6 mm. It has been found that the reconstruction method used is insensitive to the maximum viewable size limitation due to the larger probability of bubbles appearing beyond the focusing plane.[6] Nevertheless, it is advisable to use a larger field-of-view borescope that has a larger maximum viewable size limit to improve the measurement accuracy. Moreover, large bubbles have a tendency not to rise in the wall region of the column when operated in the coalesced-bubble regime.[16] This will cause a deviation from the uniform radial distribution of all bubble sizes assumption used in the reconstruction method, only near the wall region which is not important for many bubble column operations. Thus, an overestimation of the bubble size distribution may be obtained when the column is operated in the coalesced-bubble regime.

4. Conclusion

A borescope-based imaging technique, where the borescope is integrated with a statistical reconstruction method[5] and a DOF model,[6] is applied in a bubble column to study the bubble size distribution under risky elevated pressures. The statistical reconstruction method is here used to determine the actual bubble size distribution by taking into consideration the change in magnification of the bubbles at various locations from the borescope. This technique is applied in this study under a pressure range of 1 to 10 bar and a superficial gas velocity range of 20 to 50 mm/s. The bubble size distribution obtained using this technique is found to agree well with the bubble size distribution reported in literature under similar operating conditions. It has subsequently been proven that an increase in the operating pressure increases the dispersed–bubble/coalesced–bubble regime transition velocity and narrows the bubble size distribution. In summary, this study has demonstrated that borescope based imaging technique is a promising tool for bubble size measurement in bubble columns operated under elevated pressures.

Acknowledgement

Support by A*STAR SERC grant 062 101 0035 is gratefully acknowledged.

Nomenclature

Z	Axial position in the column
D	Diameter of the column
ε_G	Gas holdup
ρ	Density
P	Pressure
g	Gravity

DOF	Depth-of-field
c	Concentration
n	Coefficient
U_G	Superficial gas velocity
μ	Mean size
σ^2	Variance (wideness of size distribution)

References

[1] Bhole M R, Joshi J B and Ramkrishna D 2008 CFD simulation of bubble columns incorporating population balance modeling *Chemical Engineering Science* 63 2267-82

[2] Kulkarni A A 2007 Mass Transfer in Bubble Column Reactors: Effect of Bubble Size Distribution *Industrial & Engineering Chemistry Research* 46 2205-11

[3] Lau R, Peng W, Velazquez-Vargas L G, Yang G Q and Fan L -S 2004 Gas-Liquid Mass Transfer in High-Pressure Bubble Columns *Industrial & Engineering Chemistry Research* 43 1302-11

[4] Xue J L, Al-Dahhan M, Dudukovic M P and Mudde R F 2008 Bubble velocity, size, and interfacial area measurements in a bubble column by four-point optical probe *AIChE Journal* 54 350-63

[5] Hossain M I, Chen T, Yang Y H and Lau R. 2009 Determination of Actual Object Size Distribution from Direct Imaging *Industrial & Engineering Chemistry Research* 48 10136-46

[6] Hossain M I, Yang Y H, Borgna A and Lau R 2011 Depth-of-Field Model for Size Measurement Using a Borescope Imaging Technique under High Object Concentrations *Industrial & Engineering Chemistry Research*dx.doi.org/10.1021/ie102478q

[7] Haneishi H, Yagihashi Y and Miyake Y 1995 A new method for distortion correction of electronic endoscope images *IEEE Transactions on Medical Imaging* 14 548-55

[8] Wang G and Ching C Y 2001 Measurement of multiple gas-bubble velocities in gas-liquid flows using hot-film anemometry *Experiments in Fluids* 31 428-39

[9] Reilly I G, Scott D S, De Bruijn T J W and MacIntyre D 1994 The role of gas phase momentum in determining gas holdup and hydrodynamic flow regimes in bubble column operations *Canadian Journal of Chemical Engineering* 72 3-12

[10] Krishna R, Ellenberger J and Maretto C 1999 Flow Regime Transition in Bubble Columns *International Communications in Heat and Mass Transfer* 26 467-75

[11] Letzel H M, Schouten J C, van den Bleek C M and Krishna R 1997 Influence of elevated pressure on the stability of bubbly flows *Chemical Engineering Science* 52 3733-9

[12] Ruzicka M C, Drahos J, Fialova M and Thomas N H 2001 Effect of bubble column dimensions on flow regime transition *Chemical Engineering Science* 56 6117-24

[13] Ruzicka M C, Zahradnik J, Drahos J and Thomas N H 2001 Homogeneous–heterogeneous regime transition in bubble columns *Chemical Engineering Science* 56 4609-26

[14] Luo X, Lee D J, Lau R, Yang G Q and Fan L -S 1999 Maximum stable bubble size and gas holdup in high-pressure slurry bubble columns *AIChE Journal* 45 665-80

[15] Yang G Q, Du B and Fan L –S 2007 Bubble formation and dynamics in gas-liquid-solid fluidization - A review *Chemical Engineering Science* 62 2-27

[16] Chen R C, Reese J and Fan L -S 1994 Flow structure in a three-dimensional bubble column and three-phase fluidized bed *AIChE Journal* 40 1093-104

[17] Epstein, N., 1981, Three-phase fluidization: some knowledge gaps. *Canadian Journal of Chemical Engineering*, 59: 649.

[18] Raymond L, Rujuan M, and Wei Shan Beverly Sim *2010* Bubble characteristics in shallow bubble column reactors. *Chemical Engineering Research and Design* 88 197-203.